Journal of Ovonic Research Vol. 15, No. 2, March - April 2019, p. 135 - 141

SIZE DEPENDENT OPTICAL AND MAGNETIC PROPERTIES OF Zn DOPED IRON OXIDE NANOPARTICLES

N. RAMESH[a,b*], S. V. RANGANAYAKULU[c]
[a]*Research Scholar, Department of Physics, Rayalaseema University, Kurnool, A.P., India*
[b]*Department of Humanities & science, Marri Laxman Reddy Institute of Technology and Management, Hyderabad 500043, Telangana, India*
[C]*Guru Nanak Institutions Technical Campus(Autonomous),Ibrahimpatnam-501506, R.R.Dt, Telangana, India*

This paper presents an investigation on the Zn doped haematite nanoparticles (NPs) which were synthesized through co-precipitation route and annealed in air at different temperatures: 600 and 800^{o}C. The single phase nature has been confirmed via X-ray diffraction (XRD). The average of crystallite sizes increased progressively ranging between 33 nm and 49.7 nm as the thermal annealing increased . The obtained results confirmed the single-phase Zn doped alpha-Fe_2O_3 nanoparticles. The results of magnetic measurements made at room temperature indicate a significant improvement in the ferromagnetic order which could be understood as due to the creation of oxygen vacancies and magneto crystalline anisotropic effects due to doping. The present study indicates that doping ions may be considered as a general approach to stimulate or tune the optical and magnetic properties of nanomaterials.

(Received January 16, 2019; Accepted April 3, 2019)

Keywords: Iron oxide, Co-precipitation, Anisotropy, Optical properties, Magnetic properties

1. Introduction

Recently, nanoscale iron oxide materials have attracted intensive interest because of their potential application in high-density magnetic recording in magnetic sensors. Iron oxide, Fe_2O_3 has many phases like alpha-Fe_2O_3 (Haematite), beta- Fe_2O_3, epsilon- Fe_2O_3 and gamma-Fe_2O_3 (maghemite). Among all Fe_2O_3 oxides, Haematite, α -Fe_2O_3 is one of the most important, stable, non-toxic, nature-friendly and corrosion-resistant metal oxides. Its crystal structure is the same as that of corundum, Al_2O_3. The structure of Haematite is commonly described as rhombohedra or hexagonal with the space group $R\bar{3}c$ or D_{3d}^{6}, respectively. Its stability and low-cost mining make it the most promising natural materials in catalyst manufacturing, photo- catalysts, electrochemical and gas sensors.

Haematite undergoes a phase transition at around 260 K (Morin transition) with no net magnetic moment with a decrease in temperature [1]. Adding to the surprise it appeared to be ferromagnetic (around 1000 K) with an extremely tiny magnetic moment (0.002 μB/Fe atom), which is under considerable discussion and debate since 1950s.

In recent years, $M_xFe_{2-x}O_3$ nanoparticles have technological and scientific importance due to their new chemical and physical properties compared to bulk materials [2,3]. α-Fe_2O_3 nanostructures have been used in dye solar cells, photo-assisted electrolysis of water, active components of gas sensors, photocatalysts, ordinary catalysts, field emission, field effect transistors (FET), controlled drug delivery, lithium ion battery electrodes so on and so forth. The effect of substitution in α-Fe_2O_3 at Fe site influences the electrical, magnetic and other physical properties. In addition, several dopant species have been introduced into α-Fe_2O_3 in attempts to control materials properties [4-13], including Ti^{4+}, Si^{4+}, Nb^{5+}, V^{5+}, Al^{3+}, Zn^{2+}, and Pt^{4+}.

*Corresponding author:neelamramesh888@gmail.com

Co-precipitation method is the most helpful and attractive method for the synthesis of iron oxide nanoparticles because of its benefits likes fine stoichiometric management, the probability of obtaining ultra-fine particles in nanoscale with high crystallinity, and uniform particle distribution in short duration of time with basic laboratory equipment. Keeping in mind the above important aspects, we investigate the effect of Zinc substitution into haematite nanoparticles synthesized using co-precipitation method and study their optical as well as magnetic properties.

2. Experimental

Zn-doped haematite with chemical formula $Zn_xFe_{2-x}O_3$ (where, x=1, 0.75, 0.5, 0.25, 0(pure)) were synthesized by Co-precipitation method. Chemical reagents were of 99% purity are used without additional purification. The precursor materials $Fe(NO_3)_2.9H_2O$, $Zn(NO_3)_2.6H_2O$ and NaOH pellets were used. The weighed quantities of metal nitrates were dissolved in distilled water. Then NaOH solution is added drop wise to attain pH value of 10 and at the same time stirred by using magnetic stirrer with the speed of 400rpm, when continuous stirring of a 3-hours solution was placed singly and after a while we observed that precipitation is formed in the solution. The precipitation is separated by decanting with distilled water for several time to separate nitrates. Then precipitate was separated by filtering. Different concentrations of Zn were synthesized in same procedure. This synthesized powder was divided in two parts and heated at 600^oC and 800^oC temperatures separately.

3. Characterization

The Zn doped iron oxide nanoparticle's, The crystalline structure of pure and Zn doped iron oxide nanoparticle prepared at different annealing temperatures were examined by powder X-ray diffraction (XRD) at room temperature using CuKα radiation. The Fourier transform infrared (FTIR) spectra of these nanoparticles were recorded with varying wavelength of 400-4000 cm^{-1} using KBr pellets to verify the spinal structure of a sample. Scanning electron microscopy (SEM) is used to examine the surface morphology of these nanoparticles. To examine the magnetic properties of Zn ferrite vibrating sample magnetometer (VSM) analysis was done at room temperature.

4. Results

4.1. X-ray diffraction (XRD) analysis

X-ray diffraction (XRD) was performed to identify the phase purity, crystalline structure, and crystallinity of the materials. Fig. 1 presents the typical XRD patterns of the $Zn_xFe_{2-x}O_3$ nanoparticles calcined at 600°C and 800°C temperatures. The patterns indicate the rhombohedral structure of α-Fe_2O_3 (JCPDS card No.13-0534). No impurity phase was detected above equipment limit.

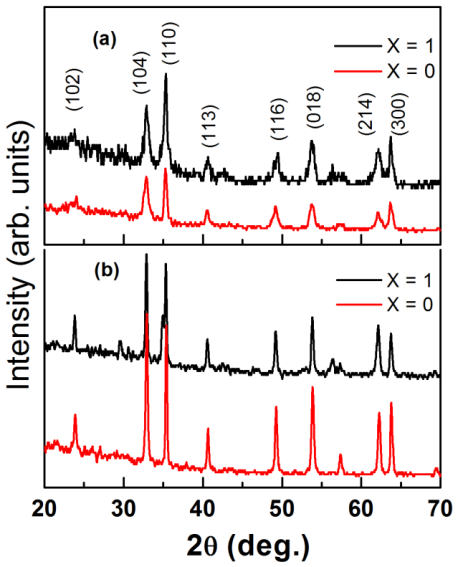

Fig. 1. Typical XRD patterns of the $Zn_xFe_{2-x}O_3$ nanoparticles calcined at (a) 600°C and (b) 800°C temperatures.

The average crystallite (grain) sizes estimated using the Scherrer's formula is given in Table 1. It can be noticed that the grain size increases with increasing annealing temperature. Furthermore, the lattice volume is observed to decrease slightly (though it cannot be considered to be significant) with the increase in Zn^{2+} content. However, the small change observed can be attributed to the creation of oxygen vacancies. Replacement of Fe^{3+} ions by Zn^{2+} ions leads to charge imbalance. In order to achieve charge neutrality, vacancy required in O^{2-} ions site and there by the lattice becomes reduced in size.

Table 1. Crystallite size of $Zn_xFe_{2-x}O_3$ (x = 0 to 1 with step of 0.25) nanoparticles prepared at 600^0C and 800^0C.

S.No	Zn content(x)	Crystallite size (nm)	
		800^0C	600^0C
1	x=1	48.6	33.5
2	x=0.75	47.2	31.1
3	x=0.5	46.7	25.6
4	x=0.25	44.7	24.1
5	x=0	41.3	24.3

4.2. Scanning electron microscopy (SEM) analysis

The Fig. 2 shows the SEM pictures of $Zn_xFe_{2-x}O_3$ samples. These micrographs show an identical distribution of particles. SEM pictures clearly reveal that the particle size will increase with the rise of temperature.

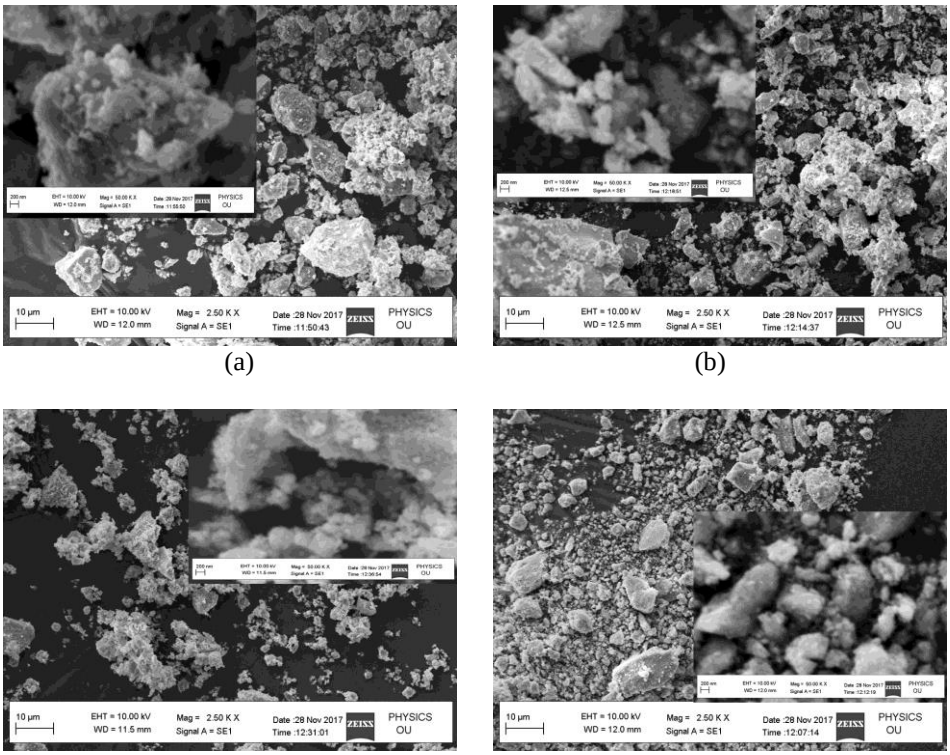

Fig. 2. Typical SEM patterns of the $Zn_xFe_{2-x}O_3$ nanoparticles calcined at 600°C (a) x = 0, (b) x =1, and calcined at 800°C (c) x = 0 and (d) x = 1.

4.3. Fourier transform infrared spectroscopy (FTIR) analysis

FTIR spectrum observed for the $Zn_xFe_{2-x}O_3$ nanoparticles are show in Fig. 3. The FTIR spectroscopy reveals the positions of ions presented within the crystal lattice by their vibrations. The FTIR spectra of nanocrystal with x=0.25,0.5,0.75,1 was recorded at room temperature within the frequency range of 4000 cm^{-1} and 400cm^{-1}. The FTIR spectroscopy results are summarized in Table 2. FTIR spectra supported the formation of a spinal structure by forming two strong bonds at around 600 and 400 cm^{-1} [11]. The ϑ1 and ϑ2 bands at 457-464 and 538-545 $cm^{-1}$are due to the Fe-O stretching vibrational modes [10].The presence of moisture (O-H group) within the sample is shown in FTIR spectra at 1635cm^{-1} and 3460 cm^{-1}, similar observation has been reported [10].

Table 2. Data on the position of FTIR absorption bands (υ1, υ2) of $Zn_xFe_{2-x}O_3$ (x = 0 to 1 with step of 0.25) nanoparticles prepared at 600^{0}C and 800^{0}C.

S.no	Zn content (x)	800^{0}C		600^{0}C	
		υ1	υ2	υ1	υ2
1	x=1	545	464	541	465
2	x=0.25	543	457	540	458
3	x=0	538	464	538	462

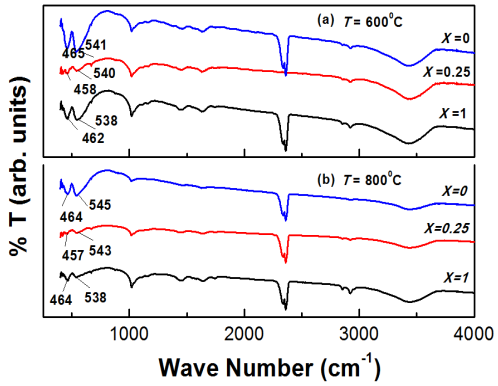

Fig. 3. FTIR spectrum for the $Zn_xFe_{2-x}O_3$ nanoparticles prepared at (a) 600°C and (b) 800°C temperatures.

4.4. Magnetic analysis

The M-H loop of $Zn_xFe_{2-x}O_3$ nanomaterial of various Zn concentrations where x=1, 0.75, 0.5, 0.25, 0 annealed at different temperatures 600°C and 800°C were measured by vibrating sample magnetometer (VSM) at maximum field of 15kOe. Fig. 4 shows typical room temperature hysteresis loops of $Zn_xFe_{2-x}O_3$(x = 0 to 1 with step of 0.25) nanoparticles annealed at 800°C. The coercive force and remanent magnetization of $ZnFe_2O_4$ nanoparticles at room temperature are negligible indicates upper paramagnetic behavior of these nanoparticles. The saturation magnetization at 15 kOe of $Zn_xFe_{2-x}O_3$ (x = 0 to 1 with step of 0.25) nanoparticles prepared at 600^0C and 800^0C are depicted in Fig. 5 and Table 3. The saturation magnetization of these nanoparticles is smaller than the bulk values. The observed saturation magnetization of these nanoparticles exhibit an increase in saturation value up to x = 0.75, beyond which it significantly diminished for both 600^0C and 800^0C annealed particles. The enhanced saturation value has been attributed to the contribution from surface anisotropy in Zn doped α-Fe_2O_3 nanoparticles. The crystalline anisotropy can be different for metal ions doped into the core of the particles and that of the surface doped particles. The anisotropy as well as the magnetic parameters is dependent on the particle size, degree of metal doping and the distribution of metal ions, and more importantly on the nature of the surface of the particles.

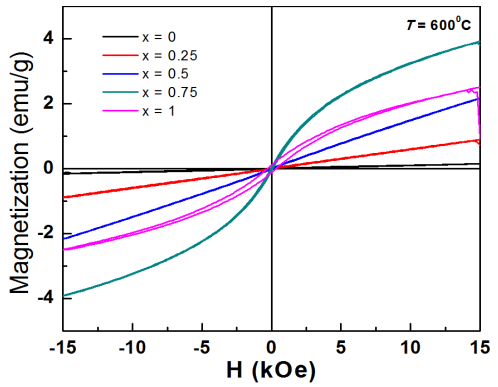

Fig. 4. Magnetic hysteresis curves of $Zn_xFe_{2-x}O_3$ (x = 0 to 1 with step of 0.25) nanoparticles prepared at 600^0C.

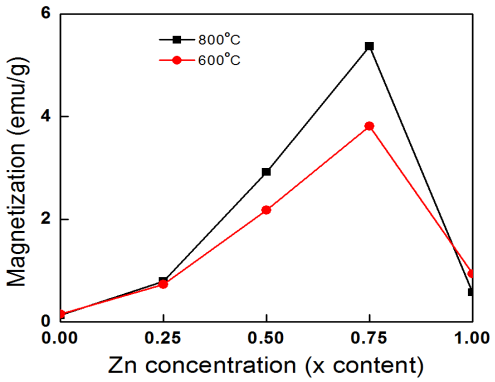

Fig. 5 Magnetization at 15 kOe of $Zn_xFe_{2-x}O_3$ (x = 0 to 1 with step of 0.25) nanoparticles prepared at 600^0C and 800^0C.

Table 3. Magnetic parameters of $Zn_xFe_{2-x}O_3$ (x = 0 to 1 with step of 0.25) nanoparticles prepared at 600^0C and 800^0C.

S.no	Zn content (x)	600^0C	800^0C
		Magnetization (emu/g)	Magnetization (emu/g)
1	x=1	0.938	0.577
2	x=0.75	3.810	5.367
3	x=0.5	2.175	2.920
4	x=0.25	0.730	0.790
5	x=0	0.152	0.134

5. Conclusions

Results of XRD, SEM and FTIR analyses indicate that the Zn doped α-Fe_2O_3 nanocrystals prepared are with good crystallinity, homogeneity, reasonably reduced grain size and high phase purity. The results of magnetic measurements made at room temperature indicates a significant improvement in the ferromagnetic order which could be understood as due to the creation of oxygen vacancies and magneto crystalline anisotropic effects due to doping. The present study indicates that doping ions may be considered as a general approach to stimulate or tune the optical and magnetic properties of nanomaterial.

Acknowledgements

One of the authors (NR) is grateful to Prof. Dibakardas, School of Engineering Sciences and Technology, Hyderabad Central University (HCU) for grant of permission to take magnetic measurements. Grateful acknowledgements to Prof G. Narasinga Rao, Marri Laxman Reddy Institute of Technology and Management for inputs and suggestions.

References

[1]P. W.Anderson, F. R. Merritt, J. P. Remeika, W. A. Yager, Phys. Rev. **93**, 717 (1954).
[2] R. Baron, F. W. Campbell, I. Streeter, L. Xiao, R. G. Compton, Int. J. Electrochem. Sci. **3**, 556 (2008).

[3] S.Mahalakshmi, K.SrinivasaManja, S.Nithiyanantham, J. Supercond. Novel Magn.**27**, 2083 (2014).
[4] A.M.Kumar, M.C.Varma, C.L.Dube,K. Rao, S.C.Kashyap, J. Magn. Magn.Mater.**320**, 1995 (2008).
[5] P.Hu, D.A.Pan,X.F. Wang, J.J.Tian, J.Wang, S.G.Zhang, A.A.Volinsky, J. Magn. Magn.Mater. **323**, 569 (2011).
[6] Y. Hwang, Materials Letters **60**, 3277 (2006).
[7] A. Rafferty, Y. Gunko, R. Raghavendra, Materials Research Bulletin**44**, 747 (2009).
[8] G. Maggioni, A. Vomiero, S. Carturan, C. Scian, G. Mattei, M. Bazzan, C.J.Fernandez, P. Mazzoldi, A. Quaranta, G.D. Mea, Appl. Phys. Lett. **85**, 5712 (2004).
[9] S.Martha, K.H.Reddy, N.Biswal, K.Parida, Dalton Trans.**41**, 14107 (2012).
[10] K. Nadeem,F.Zeba,M.A. Abid,M. Mumtaz, M.Anisur Rahman, J.Non-Cryst. Solids **400**, 45(2014).
[11] M. Akshmi, K. Vijay Kumar, K.Thyagarajan, J.Nanostruct.Chem.**5**,365(2015).
[12] D.A. Skoog, Principles of Instrumental Analysis, Saunders Golden Sunburst (1985).
[13] S.J.Stewart, S.J.A. Figueroa, M.B.Sturla, R.B.Scorzelli, F.Garcia, F.G.Requejo, Physica B, Condens.Matter.**389**, 155 (2007).
[14] G.F.Goya, H.R.Rechenberg, J. Magn. Magn.Mater.**196–197**, 191 (1999).